

## Chapter 2

### DEVELOPMENT OF RADIATION PROCESSING TO FUNCTIONALIZE CARBON NANOFIBER TO USE IN NANOCOMPOSITE FOR INDUSTRIAL APPLICATION

L. GONDIM DE ANDRADE E SILVA

Institute for Nuclear and Energy Research – IPEN/CNEN-SP,  
Cidade Universitária

M. C. EVORA

Institute for Advanced Studies- IEAV/DCTA,  
Av. Cel. Jose Alberto Albano do Amarante,  
São Jose dos Campos-SP

Brazil

#### Abstract

Radiation can be used to modify and improve the properties of materials. Electron beam and gamma ray irradiation has potential application in modifying the structure of carbon fibers in order to produce useful defects in the graphite structure and create reactive sites. In this study was investigated the methodology to functionalize carbon nanofiber (CNF) via radiation process using acrylic acid as a source of oxygen functional groups. The samples were submitted to direct grafting radiation process with electron beam and gamma source. Several parameters were changed such as acrylic acid concentration, radiation dose and percentage of inhibitor to achieve functionalization with higher percentage of oxygen functional groups on carbon nanofiber surface and better dispersion. The better results achieved was mixing CNF in a solution of acrylic acid with 6% of inhibitor ( $\text{FeSO}_4 \cdot 7\text{H}_2\text{O}$ ) and irradiated at 100 kGy. The samples were characterized by X-ray Photoelectron Spectroscopy and had an increase of 20% of oxygen content onto CNF surface. The Auger D-parameter for the samples functionalized ranged between 17.0-17.7 compared to 21.1-18.9 of the non irradiated ones. This indicated that these samples had less  $\text{sp}^2$  and more  $\text{sp}^3$  bonding characteristics than non irradiated samples. The samples functionalized presented a good and stable dispersion. Nanocomposites were manufactured from functionalized CNF and it was observed from DMA and flexural tests, an increase on the storage modulus and flexural strength. The interaction could be confirmed by SEM images where it was observed that the nanocomposites manufactured with functionalized CNF presented better interaction between functionalized CNF and resin system. The stability of the dispersion of the functionalized CNF in water during months was a good indication that the functionalization via ionizing radiation was successful.

#### 2.1. INTRODUCTION

Carbon nanofibers (CNFs) are being thoroughly investigated for application in structural composites for the aerospace industry. This requires careful control of their surfaces to promote properties required for end use, because CNFs are not compatible with most polymers.

Carbon nanofibers (CNFs) are cylindrical nanostructures composed by graphene layers that may take one of several arrangements such as stacked cones. CNFs have also attracted attention in the last ten years because they offer somewhat comparable electrical, mechanical, and thermal properties, at a lower production cost than SWCNTs and MWCNTs [2.1]. CNFs differ from SWCNT and MWCNT in the following respects: carbon nanofibers have an average diameter of 60-200 nm while carbon nanotubes have an average diameter of 10-20

nm, they are longer (30-100 micrometers) and they have a different surface morphology [2.2, 2.3].

Advanced CNFs-polymer nanocomposites can be obtained combining two specific properties: uniform dispersion of CNFs in the polymeric matrix and strong interfacial adhesion for efficient tension transfer from the polymeric matrix to the CNFs [2.4, 2.5]. Likewise CNFs, without any surface treatment, may have a weak interfacial adhesion with the polymeric matrix. Therefore, it is necessary to modify their surfaces through chemical or physical techniques to produce optimized polymer nanocomposites of a mechanical properties view.

There are several methods to functionalize carbon based materials and these modifications may promote changes on nanostructure surface [2.6-2.12]. There are some works in the literature investigating the impact of the process conditions on nanostructures and, consequently, on the technological applications of the final product. The main effects investigated are: composition of monomers and solvents employed on the functionalization [2.12-2.14], reaction temperature [2.12, 2.15], additives [2.16], and dispersion of carbon materials in solvents and water [2.17-2.19].

Radiation process, with the aim to modify carbon based materials, has been used for a long time and is a subject that still has plenty to explore [2.20-2.28]. Ionizing radiation has high enough energy to convert at least one neutral atom or molecule into an ion pair. The energy deposited by this radiation is localized in individual atoms or molecules, and it is sufficiently high to break and induce chemical reactions in a short time period. This is the basic principle of using ionizing radiation to modify materials chemically. Therefore, radiation grafting polymerization may be an alternative way to induce surface modification, and it is a uniform, effective and environment-friendly method. It can be conducted at room temperature and in gaseous, liquid and solid state phase. To date, there are some published papers related to radiation grafting polymerization to functionalize graphitic nanostructures [2.2, 2.9, 2.11, 2.22] but it still has been subject of investigation due to show a variety of structural transformations under radiation process. Adding to that, the difficulties to controlling the product are greatly magnified when the particle size is in the nanometer range. Characterization, control and reproducibility are still a challenge when particle size is in nanometer range and it is not an easy task to compare methods of characterization which are usually not in agreement with each other.

The aim of this work was to investigate and propose the methodology to functionalize CNFs and compare two different methods to promote grafting reactions: gamma ray and electron beam irradiation. Different parameters, as inhibitor concentration in acrylic acid solution, were applied to the samples during the process to establish this methodology. Fourier-Transform Infrared Spectroscopy (FTIR) and X ray Photoelectron Spectroscopy (XPS) were used to evaluate the functionalization degree of CNFs while Auger spectroscopy was used to evaluate the  $C_{sp^2}/C_{sp^3}$  ratios of CNFs comparing the different methods of irradiation. XPS and Auger spectroscopies provide an average for the content of functional groups of the first 10 – 15 molecules layer. Raman spectroscopy was used to investigate the nanostructure of carbon samples after irradiation and is a popular nondestructive tool for structural characterization of carbon materials. Scanning electron microscopy (SEM), thermogravimetric analysis (TGA), dynamic mechanical analysis (DMA) were used to characterize the functionalized samples. Composites were prepared by different methods and characterized by flexion tests and DMA.

## 2.2. EXPERIMENTAL

### 2.2.1. Carbon Nanofiber

CNFs used in this study were obtained from Applied Sciences Inc. Cedarville Ohio (under licenses from General Motors Corp. and Applied Science Inc.) and they are manufactured in a continuous vapor phase growth process that contributes to a significantly lower cost compared to most carbon nanotubes, and they are readily available in large quantities and in several grades.

CNFs (PR-25-PS grade) were selected for the investigation in this work because, in a previous work, showed less resistant under electron beam process and it was able to promote surface oxidation. Carbon nanofiber has a chemically vapor deposited (CVD) layer of carbon on the surface of the fiber over a graphitic tubular core fiber. CNFs are available in different grades. The PS grade is produced at 1100°C by pyrolytically stripping the as produced CNF to remove polyaromatic hydrocarbons from the surface.

In Table 2.1 is showed the samples submitted to direct radiation grafting process. As received PR-25-PS-XT samples were weighed, and then immersed in solutions of 10 % of acrylic acid (MERK / stabilized with 200 ppm of hydroquinone) with 1, 6 or 10 % of inhibitor metal salt ( $\text{FeSO}_4 \cdot 7\text{H}_2\text{O}$ ). One part of the samples were poured into petri dishes and irradiated with a direct accelerator operated by the Institute for Nuclear and Energy Research (IPEN/CNEN-SP/Brazil). These samples were irradiated with an industrial electron accelerator Dynamitron, from Radiation Dynamics Inc., model DC 1500/25-JOB 188 that was operated with the following parameters: beam energy 1.5 MeV, pulse current 5.62 mA, 5 kGy/pass with dose rate of 22.42 kGy/sec. Other part of the samples, with the same amount of acrylic acid and  $\text{FeSO}_4 \cdot 7\text{H}_2\text{O}$ , were irradiated by gamma radiation process in a Cobalt-60 irradiator, Gammacell model 220, series 142, manufactured by Atomic Energy of Canada Limited which activity is 64.946 TBq (1755.1 Ci) - 06/2012. The Gammacell design provides uniform gamma field and the samples were irradiated at a dose rate of 1.48 kGy/h. The mixtures were purged with dry nitrogen for 10 min to remove dissolved oxygen and then sealed.

TABLE 2.1. SAMPLES PREPARED WITH ACRYLIC ACID SUBMITTED TO DIRECT RADIATION GRAFTING PROCESS

Samples Name	Samples PR-25-PS-XT	Dose (kGy)		$\text{FeSO}_4 \cdot 7\text{H}_2\text{O}$ (%)
GA-1	pristine	0	-	None
Blank-1	pristine	0	-	1 %
Blank-2	pristine	0	-	6 %
GA-11	pristine	50 kGy	e-beam	6 %
GA12	pristine	100 kGy	e-beam	6 %
GA-13	pristine	100 kGy	gamma	6 %
GA-14	pristine	100 kGy	gamma	10%
GA-16	pristine	90 kGy	gamma	6 %
GA-17	pristine	90 kGy	e-beam	6 %
GA-18	Pre-irradiated at 1000 kGy	90kGy	e-beam	6 %

The surface oxygen content of the nanofibers was characterized with X-ray Photoelectron Spectroscopy (XPS) analysis. GA-1, Blank-1, GA 12, GA-13 and GA-14 were conducted in K- Alpha XPS equipment from ThermoFisher Scientific, with a 400  $\mu\text{m}$  X-ray spot size and with the low energy electron/argon ion charge neutralization system turned on. XPS survey spectra (0-1350 eV) were collected for all samples to provide qualitative and quantitative

surface analysis information. The XPS analysis for GA-1, Blank-2, GA-16, GA-17 and GA-18 were carried out in National Institute of Metrology, Quality and Technology (Inmetro). X-ray photoelectron spectroscopy (ESCAplus P System; Omicron Nanotechnology; Taunusstein, Germany) was used in order to study the chemical composition and chemical groups in carbon nanofibers before and after an irradiation process. The XPS analyses were performed in an ultra-high vacuum medium using an Al K $\alpha$ =1486.7 eV X-ray source, with a 20 mA emission at a voltage of 13.5 kV. Survey spectra were acquire in the range of 1350-0 eV, step of - 0.8 eV, dweel time of 0.2 eV, and resolution of 70 eV. For carbon and oxygen elements, the high resolution spectra were obtained with analyzer pass energy of 30 eV. The binding energies were referenced to the carbon 1s level at 284.6 eV. The Shirley background and a least-squares routine, as implemented in the Casa XPS software (licensed by Omicron Nanotechnology, Taunusstein, Germany), were used for peak fitting. The FTIR analyses were performed in a Perkin-Elmer Spectrum GX spectrometer (Perkin-Elmer, Massachusetts, USA) by the potassium bromide (KBr) transmission technique.

### 2.2.2. Nanocomposites

The great difficulty that exists in the manufacture of nanostructured composite is the dispersion of CNF in the matrix. These materials have basically non-polar surfaces. There is a necessity to make changes on the surface which allows better interaction and dispersion in the polymer matrix of interest. In the present investigation, two different dispersion processes were performed with the aim to study the best process to manufacture the nanocomposites and with the modified CNF. The processes are:

- Mix nanofiber/matrix - Conventional Process
- 3 roll mill dispersion process

#### 2.2.2.1. Mix nanofiber/matrix - Conventional Process

The epoxy system used in the development of this experiment was also Araldite GY 260 and HT 972 curing agent in ratio of 80g of resin and 21.6g of hardener. This amount was sufficient to manufacture samples with 100x14x4mm approximately (Figure 1.1). The resin and hardener were mixed on a hot plate at 100°C until the system becomes homogeneous. 0.508g of CNF was added to the resin system. The compound mixture was placed in a vacuum oven to remove bubbles and then poured into the metal mold which was prior treated with mold release agent. The material was cured in a vacuum oven and a cure ramp according to the schedule shown in Table 2.2. The composition of the composites obtained by the conventional method is described in Table 2.3 and the manufactured composite are presented in Fig. 2.1.

TABLE 2.2. CURING PROCESS OF NANOCOMPOSITES PREPARED BY CONVENTIONAL METHOD

Time	Temperature
30 minutes	110°C
1 hour	120°C
2 hours	140°C
1 hour e 30 minutes	160°C
2 hours	180°C

TABLE 2.3. COMPOSITION OF NANOCOMPOSITES PREPARED BY CONVENTIONAL METHOD

Samples	Composition
BANC1-1	Bisphenol A + curing agent
1NC1-1	Bisphenol A + curing agent + 0,5% de CNF GA1
15NC1-1	Bisphenol A + curing agent + 0,5% de CNF GA15
16NC1-1	Bisphenol A + curing agent + 0,5% de CNF GA16
17NC1-1	Bisphenol A + curing agent + 0,5% de CNF GA17
18NC1-1	Bisphenol A + curing agent + 0,5% de CNF GA18

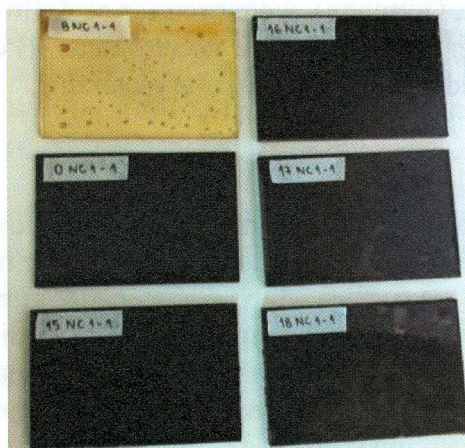


FIG. 2.1. Nanocomposites manufactured via a conventional method.

#### 2.2.2.2. 3 roll mill dispersion

The epoxy system filled with CNF functionalized and non-functionalized were prepared by shear process dispersion using a 3-roll mill adapted for this function. This process was researched and developed at the University of Dayton (Fig. 2.2).



FIG. 2.2. Three roll mill dispersion at composites carried out at University of Dayton Lab.

The epoxy system used consists of Epon 862 (bisphenol F) and curing agent Epikure W (26 wt%). Both kindly provided by the University of Dayton in collaboration with this project. In each composite it was used 160g of resin and curing agent 42.24g. The mold used for composites manufacture is formed by two plates of the following dimensions: 10x10x0.7cm (Fig. 2.3) and the amounts of each mixture were enough prepared to fill the mold. The epoxy resin system was premixed in a vessel containing 0.5% of functionalized and non functionalized CNF. The mixture was then dispersed in a 3 roll mill as it is shown in Figure 2.2. The mixture was processed in the 3 roll mill for 5 times until the CNF was fully dispersed.

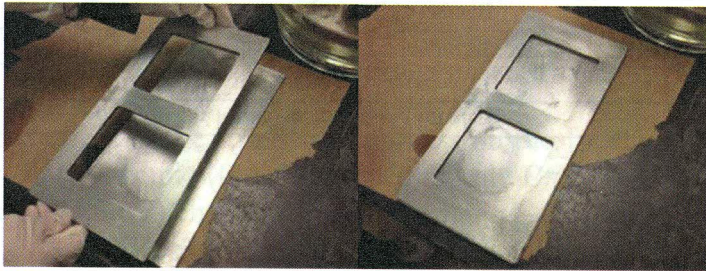


*FIG. 2.3. Mold used at the University of Dayton for making nanostructured composites.*

This mixture was poured in a previously sprayed with mold release agent and the mold was placed in a hot press (Fig. 2.4) under a pressure of 7 tons. The samples were cured according to the curing process shown in Table 2.4 and the compositions of the composites obtained by shear process are presented in Table 2.5.



*FIG. 2.4. Hot press used to manufacture nanocomposites at University of Dayton.*

TABLE 2.4. CURING PROCESS OF NANOCOMPOSITES PREPARED BY SHEAR METHOD

Time	Temperature
1 hour	120°C
2 hours	180°C

TABLE 2.5. COMPOSITION OF NANOCOMPOSITES PREPARED BY 3 ROLL MILL METHOD

Samples	Composition
BFNC1-2 (M)	Bisphenol F + curing agent
1NC1-2 (M)	Bisphenol F + curing agent + 0,5% de NFC GA1
15NC1-2 (M)	Bisphenol F + curing agent + 0,5% de NFC GA15
16NC1-2 (M)	Bisphenol F + curing agent + 0,5% de NFC GA16
17NC1-2 (M)	Bisphenol F + agente de cura + 0,5% de NFC GA17

### 2.3. RESULTS AND DISCUSSION

Fig.2.5. shows the results of the dispersion of the samples GA-15 (blank 2), GA-16, GA-17 and GA-18. The samples were dispersed in water under sonication process for an hour. This picture was taken 70 days after the dispersion process.

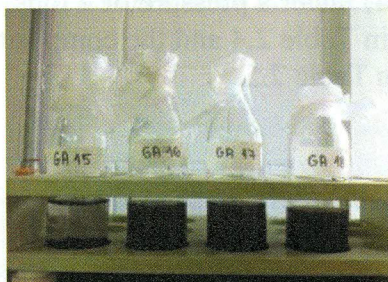


FIG. 2.5. Illustration of Blank-2, GA-16, GA-17 and GA-18 dispersed after 70 days.

XPS survey spectra (0-1350 eV) were collected for all samples to provide qualitative and semi-quantitative surface analysis information, Table 2.6. The O/C atomic ratios calculated from XPS survey spectra are an important feature in order to compare non irradiated and irradiated samples. The increase of the O/C atomic ratio is an indication of the effectiveness of the grafting process. The surface composition (atomic %) showed a significant increase of oxygen content for the samples irradiated, and for this reason, they offer excellent and very stable dispersion.

TABLE 2.6. SURFACE COMPOSITIONS (ATOMIC %) AND O/C ATOMIC RATIOS CALCULATED FROM BY THE XPS SURVEY SPECTRA (SEE METHODS) FOR CARBON NANOFIBERS AS RECEIVED (GA-1), NON-IRRADIATED SAMPLES (BLANK-1 AND BLANK-2) AND IRRADIATED SAMPLES (GA11, GA12, GA13, GA14, GA16, GA17 AND GA18)

at (%)	GA-1	Blank 1*	Blank 2	GA 11*	GA 12*	GA 13*	GA 14*	GA 16	GA 17	GA 18
C	93.1	90.6	90.2	83.1	79.7	78.4	81.5	80.6	68.3	82.9
O	5.1	7.0	7.6	14.6	18.4	20.3	16.8	18.4	30.7	15.8
N	1.1	1.6	1.4	1.4	0.9	0.9	0.9	0.6	0.5	0.9
Fe	0.1	0.1	0.2	0.1	0.1	0.1	0.2	0.1	0.1	0.1
S	0.5	0.4	0.5	0.4	0.3	0.2	0.4	0.2	0.3	0.2
Si	0.1	0.3	0.1	0.4	0.1	0.1	0.2	0.1	0.1	0.1
O/C	0.04	0.06	0.06	0.13	0.17	0.19	0.15	0.17	0.34	0.14

\* Analyzed in K- Alpha XPS equipment from Thermo Fisher Scientific.

Figure 2.6. shows the effect of the irradiation process on the functionalization of the carbon nanofibers. Non irradiated sample (GA-1) showed mainly C=C, C-H bounds and a shake-up satellite peak ( $\pi \rightarrow \pi^*$ , 291.3 eV) characteristic of aromatic C structures [2.29-2.31]. A binding energy of 284.3 eV essentially corresponds to non-functionalized  $sp^2$  carbons which would be expected for CNF materials [2.29]. The sample irradiated with 100 kGy of gamma radiation (GA-13) showed more intensity in the peak characteristic of O-C=O bound ( $\sim 289.3$  eV) than the sample irradiated with the same dose of e-beam (GA12) which may be an indication that the grafting process was more effective using gamma radiation. These two radiation sources promotes different primary event of interaction with the matter however for both, secondary electron is responsible to initiate the ionization events that produce free radicals. On the other hand, electron beam delivers much higher dose rate leading to heating and contribute to generate various rearrangements of the carbon atoms.

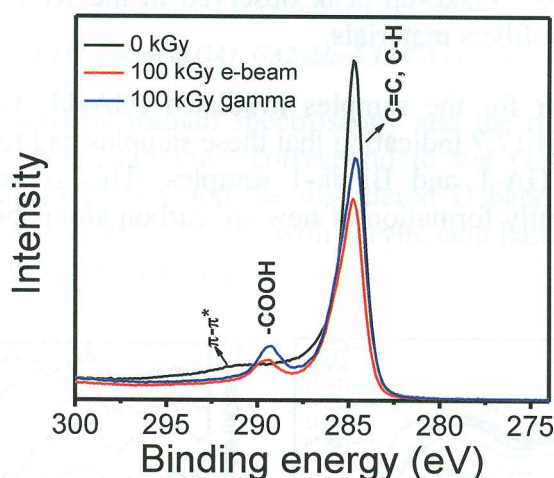


FIG. 2.6. XPS spectra of C1s of PR-25-PS pristine, non irradiated (GA-1) and irradiated with 100 kGy of e-beam (GA-12), and irradiated with 100 kGy of gamma radiation (GA-13). Both samples were analyzed in K- Alpha XPS equipment from ThermoFisher Scientific.

The effect of the irradiation doses on the graphitization level of the carbon nanofibers is showed in Fig. 2.7. In Fig. 2.7a, the samples irradiated with e-beam showed an increase in the intensity of carboxyl peak with the increase of the irradiation dose. For the samples irradiated

with gamma radiation, Fig. 2.7b, the samples irradiated with 90 and 100 kGy showed similar behavior relative to graphitization process evidenced by the carboxyl peak intensities.

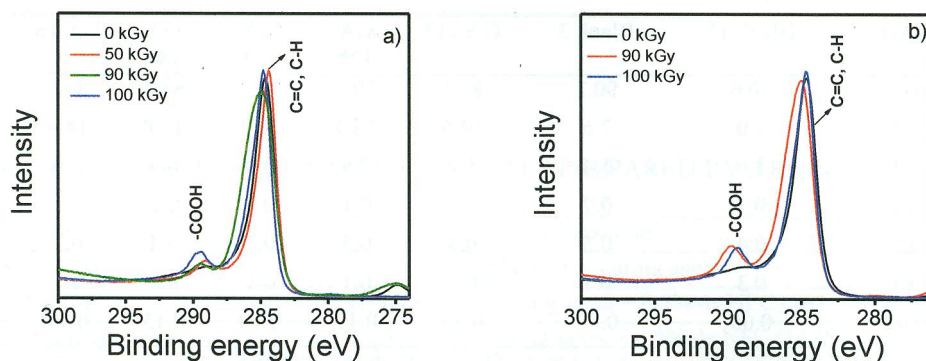


FIG. 2.7. XPS spectra of C1s of PR-25-PS with 6% of inhibitor ( $\text{FeSO}_4 \cdot 7\text{H}_2\text{O}$ ), where: a) irradiated with different doses of e-beam radiation (0, 50, 90 and 100 kGy). These samples correspond to Blank-2, GA-11, GA-12 and GA-17 in table 2.1; b) irradiated with different doses of gamma radiation (0, 90 and 100 kGy). These samples correspond to Blank-2, GA-16 and GA-13 in Table 2.1.

The X-ray induced CKLL Auger spectra were similar for the six samples (Fig. 2.8a) but did show some minor differences in peak shape and position. It has been shown in the published literature that, after differentiation, C KLL Auger spectra can give important information regarding the relative amount of  $\text{sp}^2$  and  $\text{sp}^3$  bonding in carbon materials by the so called Auger "D-parameter" [2.32]. The C KLL data were differentiated to give the Auger "D-parameter," which is the energy separation between the primary "hill" and "valley" of the differentiated spectrum. The D-parameter value gives an indirect measure of the %  $\text{sp}^2$  character of the material. The measured Auger D-parameter for Sample GA-1 was 21.6 (Fig. 2.8b), similar value to the literature reference for graphite [2.32]. This result indicates a significant amount of  $\text{sp}^2$  bonding on the surface of the non-irradiated sample, which is consistent with the  $\pi \rightarrow \pi^*$  shake-up peak observed in the XPS C1s peak fit results, and is expected for carbon nanofibers materials.

The Auger D-parameter for the samples irradiated (GA-11, GA-12, GA-13 and GA-14) ranged between 17.0 and 17.7 indicating that these samples had less  $\text{sp}^2$  and more  $\text{sp}^3$  bonding compared to samples GA-1 and Blank-1 samples. This is an indication of C=C bond breaking, and subsequently formation of new  $\text{sp}^3$  carbon atoms on CNT surface with oxygen functional groups.

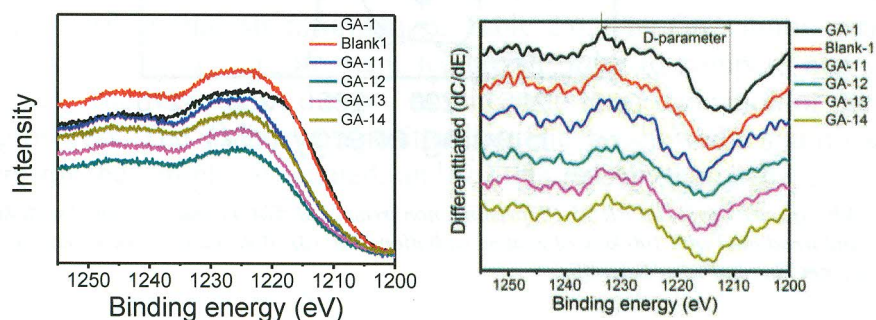


FIG. 2.8. (a) Raw Auger data of carbon nanofibers samples pristine (GA-1, Blank-1) and irradiated samples (GA-11, GA-12, GA-13 and GA-14); (b) Differentiated Auger spectra and Auger D-parameter for PR-25-PS grafted with acrylic acid  $^{60}\text{Co}$   $\gamma$ -rays and industrial electron accelerator.

FTIR spectra of carbon nanofibers are shown in Fig. 2.9. FTIR is a very useful technique to investigate the functional groups attached to the surface of carbon nanofibers. The peaks in the 2805-3010  $\text{cm}^{-1}$  region are characteristic of C-H stretching, and their intensities are enhanced after functionalization process (GA-1 and Blank-1 compared with GA-11, GA-13 and GA-14), which can be explained by the attachment of alkyl groups onto the surface of carbon nanofibers and the increase of defects by irradiation [2.33]. Vinyl bounds (C=C) stretching vibrations appear in  $\sim 1640 \text{ cm}^{-1}$  and are typically from aromatic compounds. The radiation incidence on the carbon nanofibers promotes crosslinking of C=C terminal bounds, transforming  $\text{Csp}^2$  in  $\text{Csp}^3$  bounds. A peak at  $\sim 1090 \text{ cm}^{-1}$  in GA-11, GA-13 and GA-14 may be ascribed to the C-O stretching mode, indicating the presence of hydroxyl groups in samples irradiated. The peak around  $1740 \text{ cm}^{-1}$  can be assigned to the stretching mode of carbonyl groups present in the functionalized samples, indicating the presence of polyacrylate (PAA) chains in carbon nanofibers. In addition, a broad band in the  $3100\text{-}3600 \text{ cm}^{-1}$  region is attributed not only to the presence of hydroxyethyl group and PAA chains containing OH, but also to traces of water in the KBr used for the analysis which is inaccessible to be fully removed.

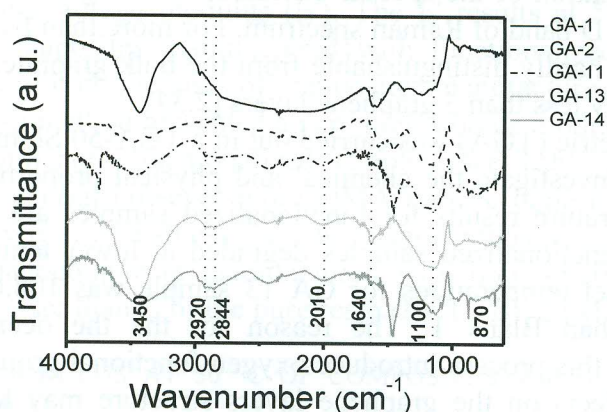


FIG. 2.9. FTIR spectra of GA1, GA2 (blank), GA 11, GA 13 and GA 14.

The samples were characterized by Raman spectroscopy and the results are shown in Fig. 2.10. The peaks near  $1575$  and  $1325 \text{ cm}^{-1}$  correspond to the G band due to stretching vibrations of the  $\text{sp}^2$ -hybridized carbon and the disordered D band attributed to defective carbon atoms, respectively. The samples treated with acrylic acid had the D frequency shifted to left  $5.5 \text{ cm}^{-1}$  and G frequency did not change.

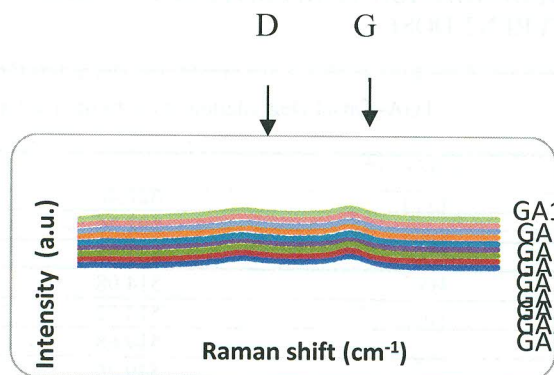


FIG. 2.10. Raman spectroscopy results of PR-25-PS irradiated at  $1000 \text{ kGy}$ , soaked into monomers solution with water/methanol (50% vol) and washed with deionized water to remove the residual monomers and by products.

The Raman spectra of all carbons showed several common features in the 800-2000  $\text{cm}^{-1}$  region, called G and D peaks, which lie around 1560 and 1360  $\text{cm}^{-1}$ . The intensity ratio of D band to G band in the Raman spectra has been widely used to evaluate the defects in carbon nanomaterials. The increase of ID/IG ratios may indicate generation of defects on carbon nanofiber surface due to the covalent bonding formation with functional groups grafted on carbon nanofiber surface. The results presented in Figure 2.10. showed that there are no meaningful changes in the carbon nanofiber structure. High radiation dose was not able to damage the bulk CNF structure. It was localized to the surface and did not compromise the core of the carbon nanofiber. Thus, the advantage of this process is that the overall graphitic structure has not been damaged. The radiation grafting reaction is carried out on external layer, which is less organized than the bulk of the wall. Raman spectroscopy is a bulk characterization technique in which the laser penetration ( $\sim 1 \mu\text{m}$ ) may exceed the thickness of the turbostratic carbon layer deposited on the nanofiber surface where the oxidation takes place. In general, the graphite structure of the nanofiber core did not show any damage.

Generally the Raman spectra of carbon materials are simple, with two most intense bands between 1000 and 2000  $\text{cm}^{-1}$ . The dispersion of  $\pi$  electrons in graphene is why Raman spectroscopy is always resonant for carbon. However, Raman has some drawbacks that may lead to misinterpretation of the spectra. Ferrati A. investigated the impact of multiple layers of graphene on the D band of Raman spectrum. For more than five layers, the D band Raman spectrum becomes hardly distinguishable from the bulk graphite. Thus Raman spectroscopy can clearly identify less than 5 graphene layers [2.34].

The thermogravimetric (TGA) was carried out in a TGA-50 Shimadzu equipment and it is an important tool to investigate the chemical and physical properties of a material. The onset degradation temperature results for functionalized samples are presented in Table 2.7. It showed that the functionalized samples degraded at lower temperature. For instance, the decomposition onset temperatures for GA 13 sample was 108.68  $^{\circ}\text{C}$  lower than GA1 and 78.54  $^{\circ}\text{C}$  lower than Blank 1. The reason for the decrease of onset degradation temperature is that this process introduces oxygen functional groups covalently bonded on CNF surface. These defects on the graphene layers structure may lower the onset degradation temperature of the samples. The thermal stability of non-irradiated CNF (GA1, blank 1 and blank 2) was higher than the irradiated ones. This stability can be attributed to the degree of defects and damages (see Table 2.7. and Fig. 2.11a and 2.11b). The non-irradiated sample (GA1, blank 1 and blank 2) began to lose mass between 550 and 622 $^{\circ}\text{C}$ , which was attributed to impurities or imperfections in the nanofiber and the functionalized samples, starts to lose weight around 250 $^{\circ}\text{C}$ . In addition, the irradiated samples exhibited a more pronounced weight loss from 500-800 $^{\circ}\text{C}$  than non-functionalized carbon nanofibers.

TABLE 2.7. ONSET DEGRADATION TEMPERATURE FOR SAMPLE IRRADIATED IN IPEN FACILITIES AT DIFFERENT DOSE

Dose	TGA- Onset Degradation temperature ( $^{\circ}\text{C}$ ), (10 $^{\circ}\text{C}/\text{min}$ in $\text{N}_2$ )
GA1	622.40
Blank 1	592.26
GA11	535.57
GA11.1	514.08
GA 13	513.72
GA14	519.68
Blank 2	549.26
GA17	527.83
GA18	527.91

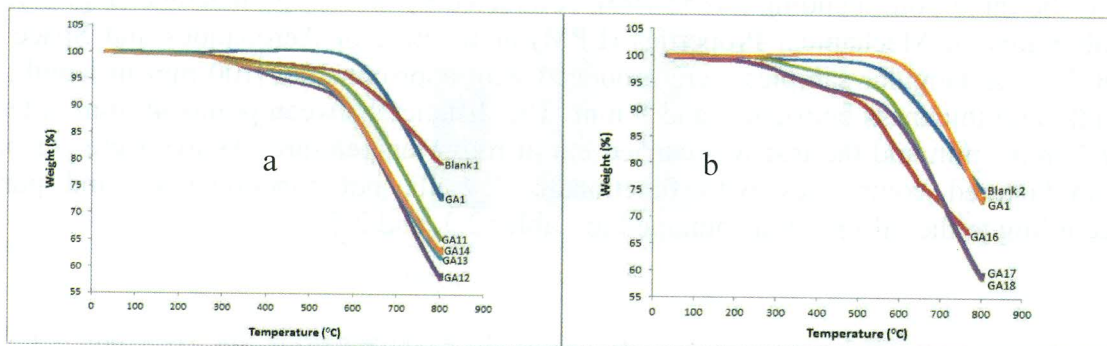


FIG. 2.11. TGA for non functionalized and functionalized samples.

The DMA results are very sensitive to changes in structure of materials. The DMA analyses are being carried out in a TA Instruments model DMA 2980, operating at a frequency of 1 Hz in a temperature range from 20 to 200 °C at a heating rate of 2 °C/min. The analyses were conducted at the Laboratory of the Division of Materials DCTA. The viscoelastic properties were evaluated mainly by the storage modulus ( $E'$ ). The  $E'$  results at 50 °C are shown in Tables 2.8. and 2.9. The composites manufactured with functionalized CNF showed an increase in storage modulus in both methods of composites manufacture. The 16NC1-2 (M) sample prepared by 3 roll mill method presented a very high storage modulus when compared to nanocomposites made with non- functionalized samples (see Table 2.9). It may be an indication of rigidity of the material however more DMA will be done to verify this result. Overall, there is an increase of stiffness on the nanocomposites manufactured with functionalized CNF. The nanocomposite manufactured with non functionalized CNF (15 CNF -2 NC1 (M)) has a  $E'$  lower than  $E'$  of the pure resin (NC1 - BF 2 (M)).

TABLE 2.8. ELASTIC MODULUS AT 50 °C OF COMPOSITES MANUFACTURED BY THE CONVENTIONAL METHOD

Samples	$E'$ (MPa)
BANC1-1	1732
INC1-1	1605
15NC1-1	1600
16NC1-1	1871
17NC1-1	2173
18NC1-1	1823

TABLE 2.9. ELASTIC MODULUS AT 50 °C OF COMPOSITES MANUFACTURED BY THE 3 ROLL MILL METHOD

Samples	$E'$ (MPa)
BFNC1-2 (M)	1714
INC1-2 (M)	1740
15NC1-2 (M)	1604
16NC1-2 (M)	8993
17NC1-2 (M)	1873

The mechanical properties were investigated so far by flexural test. The flexural test adopted was the three-point bending (ASM 790), conducted by an Instron machine (Fig. 2.12) in the Laboratory of Mechanical Properties (LPM) at Institute of Aeronautics and Space (IAE) / DCTA. Rectangular samples were produced with approximately 100 mm in length, 14 mm width and thickness between 3 and 5 mm. The distance between points 40 mm, a test speed of 1 mm / min and the test was carried out at room temperature. Assays were performed in manufactured composites with functionalized CNF, not functionalized and pure resin according to the information contained in Tables 2.3. and 2.5.

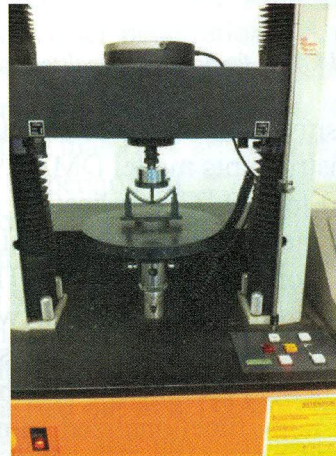


FIG 2.12. – Instron machine - flexural test.

As illustrated in Fig. 2.13. and 2.14., the composites manufactured with functionalized CNF had flexural strength higher than those of composites manufactured non-functionalized CNF. More flexion tests should be performed in order to have good statistic of the results. Comparing the samples 16NC1 -1 and 16NC1-2 (M) it can be observed an increase on flexural strength which can be attributed to the manufacturing process of the composite. 3 roll mill process promotes better interaction CNF/ epoxy. At the same time, the process leads to a shearing wear surface and this can be a disadvantage for samples irradiated by the electron beam that promotes more damages on CNF surface due to electron beam energy and high dose rate compared to gamma radiation. This results is in accordance with DMA, the 17NC1 -2 (M) sample presented lower E' than the 16NC1 -2 (M).

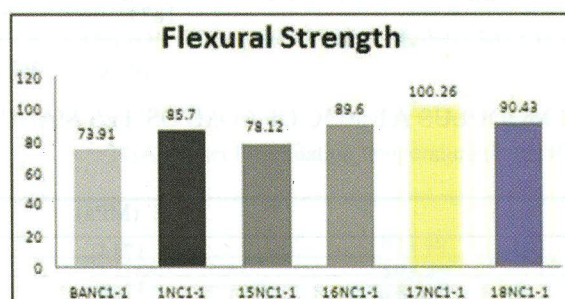


FIG. 2.13. Flexural strength of composites manufactured by convencional method.

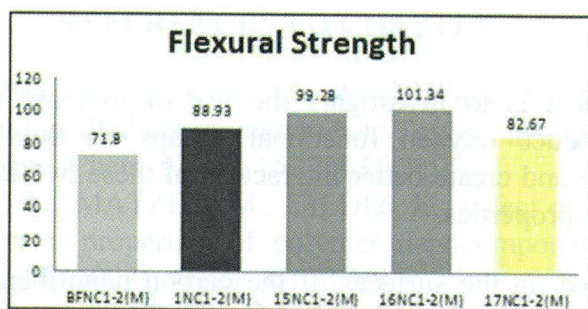


FIG. 2.14. Flexural strength of composites manufactured by 3 roll mill method.

In Fig. 2.15. and 2.16. are shown images of SEM. The morphology of the nanocomposites was analyzed in Magellan model microscope from Federal University of São Carlos in the State of São Paulo. The SEM images of nanocomposites made with GA1 and blank 2 carbon nanofiber are shown in Figure 2.15a and 2.15b. Investigating the morphology of nanocomposites samples, it was observed that the samples presented detachments from the resin system (Fig. 2.15a and 2.15b). The nanocomposites manufactured with functionalized carbon nanofibers presented more molhability and attachment with the resin.

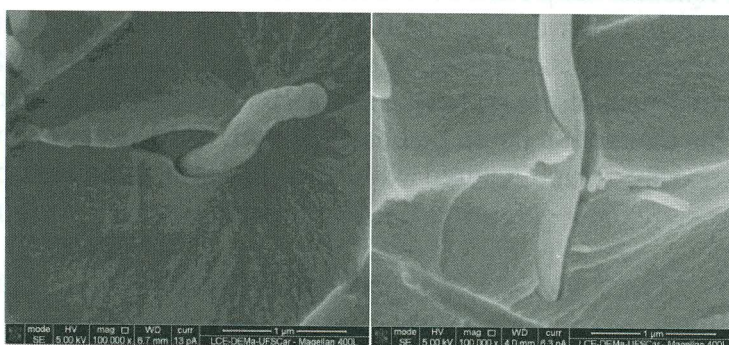


FIG. 2.15. SEM images of non irradiated samples a- nanocomposites manufactured with GA1 and b- nanocomposites. manufactured with blank2.

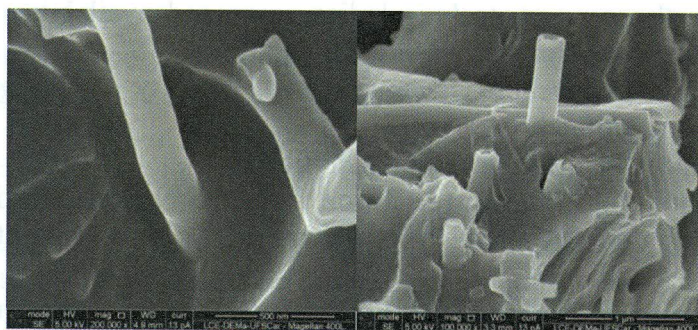


FIG. 2.16. SEM images of irradiated samples a- nanocomposites manufactured with GA16.

## 2.4. CONCLUSION

The aim of this project is to investigate the use of ionizing radiation to developing a methodology to introduce oxygen functional groups on the CNF surface to improve fiber/matrix dispersion and create better interaction of these two compounds aiming to make composites with better properties.

The changes performed on the surfaces of the carbon nanofibers via ionizing radiation to graft functional groups were successfully performed. The methodology was established and the process was reproducible. We observed that the changes occurred on CNF surface and XPS results showed a significant increase in the percentage of oxygen in the CNF surface.

Two methods investigated to manufacture nanocomposites with functionalized CNF. Overall, the application of these functionalized nanofibers in composites showed promising results. The best results seem to be those that were made by 3 roll mill method. Despite the difficulties that each manufacture methodology, the 3 roll mill process was the most efficient process for providing composites with less bubbles and promoted greater interaction between functionalized nanofiber and the polymer matrix. From the results of DMA and flexural tests, it was observed an increase on the storage modulus and flexural strength on the nanocomposites manufactured with CNF functionalized. The stability of the dispersion of the functionalized CNF in water during months was a good indication that the functionalization via ionizing radiation was successful, it can be suggest that the functionalized nanofiber promoted better interface in the composites analyzed, but different mechanical tests will still be conducted. This interaction could be observed with SEM technique where it was observed that the nanocomposites manufactured with CNF non functionalized presented detachments from the resin system.

## ACKNOWLEDGEMENTS

We would like to acknowledge the International Atomic Energy Agency the support to this project as well as we would like to thanks the collaborators such as :

- Dr Luis Claudio de Moura Pardini and Andreza Cardoso Institute of Aeronautics and Space DCTA for the support, technical discussion and collaborations during this project.
- Elizabeth Somessari and Carlos Gaia da Silveira from Institute for Nuclear and Energy Research for the support, technical discussion and availability for the irradiation process which is the main tool for this research project.
- Dr. Tony Saliba and Deborah Daloia from University of Dayton for the technical support on composites manufacturing.
- •Applied Sciences Inc. for the carbon nanofiber.
- Dr. Joyce Araujo and Dr. Martins Erlon from the National Institute of Metrology, Quality and Technology (INMETRO) by important analyzes and investigations conducted during the technical visits.
- Dr Brian Strohmeier Thermo Fisher Scientific by XPS analysis that were important to verify the reproducibility of the method established performed.
- At the Institute for Advanced Studies would like to thank Mr David Neves analysis by X-ray diffraction and the design of the molds for composites. SUTEC colleagues from the implementation of this project and Dr. Raquel Villela of Nuclear Energy Division for technical support. And finally, I thank the student Marina Gorgulho for her work on the project tasks.

## REFERENCES TO CHAPTER 2

- [2.1] EITAN, A., JIANG, K., DUKES, D., ANDREWS, R., Schadler, L., Surface modification of multiwalled carbon nanotubes: Toward the tailoring of the interface in polymer composite, *Chem. Mater.* 15 (2003), 3198.
- [2.2] LAFDI, K., FOX, W., MATZEK, M., YILDIZ, E., Effect of carbon nanofiber heat treatment on physical properties of polymer nanocomposites, Part I, *Journal of Nanomaterials v 2007 (2007)*, Article ID 53729.
- [2.3] LAFDI, K., FOX, W., MATZEK, M., YILDIZ, E., Effect of carbon nanofiber-matrix adhesion on polymer nanocomposite properties- Part II, *Journal of Nanomaterials, 2007 (2008)* Article ID 53729.
- [2.4] YU, H., MO, X. et al., Radiation-induced grafting of multi-walled carbon nanotubes in glycidyl methacrylate-maleic acid binary aqueous solution, *J Phys.Chem.* 77 (2008) 656.
- [2.5] PEDRONI, L. G., ARAUJO, J. R., FELISBERTI, M. I., NOGUEIRA, A.F., Nanocomposites based on MWCNT and styrene-butadiene-styrene block copolymers: Effect of the preparation method on dispersion and polymer-filler interactions, *Composites Science and Technology* 72 13 (2012) 1487.
- [2.6] LONG, D., WU G, ZHU G., Noncovalently modified carbon nanotubes with carboxymethylated chitosan: A controlled donor-acceptor nanohybrid, *Int. J. Mol. Sci.* 9 (2008) 120.
- [2.7] ZHANG X., SREEKUMAR T.V., LIU T., KUMAR S., Properties and Structure of Nitric Acid Oxidized Single Wall Carbon Nanotube Films, *J. Phys. Chem. B* 108 (2004) 16435.
- [2.8] WANG S., LIANG Z., LIU T., WANG B., ZHANG C., Effective amino-functionalization of carbon nanotubes for reinforcing epoxy polymer composite, *Nanotech.* 17 (2006) 1551.
- [2.9] PAREDES J.I., MARTINEZ-ALONSO A., TASCÓN J.M.D., Oxygen plasma modification of submicron vapor grown carbon fibers as studied by scanning tunneling microscopy, *Carbon* 40 (2002) 1101.
- [2.10] SHIN Y., JEON I., BAEK J., Stability of multi-walled carbon nanotubes in commonly used acidic media, *Carbon* 50 (2012) 1465.
- [2.11] BRUSER V. et al, Surface modification of carbon nanofibers in low temperature plasmas, *Diamond Relat. Mater.* 13 (2004) 1177.
- [2.12] WEI G., SHIRAI K., FUJIKI K., SAITOH H., YAMAUCHI T., TSOBOKAWA N., Grafting of vinyl polymers onto VGCF surface and the electric properties of the polymers-grafted VGCF. *Carbon* 42 (2004) 1923.
- [2.13] CHOI S., NHO Y.C., Radiation-Induced Graft Copolymerization of Mixture of Acrylic Acid and Acrylonitrile onto Polypropylene Film, *Korea Polym. J.* 64 (1998) 287.
- [2.14] CHAUDHARI C.V., BHARDWAJ Y.K., SABHARWAL S., Radiation grafting of methyl methacrylate on radiation crosslinked natural rubber film, *J. Radioanal. Nucl. Chem.* 267 1 (2006) 113.
- [2.15] CHEN J., WEI G., MAEKAWA Y., YOSHIDA M., TSOBOKAWA N., Grafting of poly(ethylene-block-ethylene oxide) onto a vapor grown carbon fiber surface by  $\gamma$ -ray radiation grafting, *Polymer* 44 (2003) 3201.
- [2.16] CHEN J., WEI G., MAEKAWA Y., YOSHIDA M., TSOBOKAWA N., Grafting of poly(ethylene-block-ethylene oxide) onto a vapor grown carbon fiber surface by  $\gamma$ -ray radiation grafting, *Polymer* 44 (2003) 3201.

- [2.17] CHEN S. et al., Preparation of Poly(acrylic acid) Grafted Multiwalled Carbon Nanotubes by a Two-Step Irradiation Technique. *Macromolecules* 39 (2006) 330.
- [2.18] JUNG C., KIM D., CHOI J., Surface modification of multi-walled carbon nanotubes by radiation-induced graft polymerization, *Curr. Appl. Phys.* 9 (2009) 85.
- [2.19] MARTÍNEZ-HERNÁNDEZ A., VELASCO-SANTOS C., CASTAÑO V.M., Carbon Nanotubes Composites: Processing, Grafting and Mechanical and Thermal Properties, *Curr. Nanosci.* 6 (2010) 12.
- [2.20] CLOCHARD M.C., BEGUE J., LAFON A., CALDEMAISON D., BITTENCOURT C., PIREAUX J., BETZ N., Tailoring bulk and surface grafting of poly(acrylic acid) in electron-irradiated PVDF, *Polymer* 45 Issue 25 (2004) 8683.
- [2.21] CHEN J., MAEKAW, Y., YOSHIDA M., TSOBOKAWA N., Radiation grafting of polyethylene onto conductive carbon black and application as a novel gas sensor, *Polym. J.* 34 n 1 (2002), 30.
- [2.22] CHEN X. et al. In-Situ X-ray Scattering Studies of a Unique Toughening Mechanism in Surface-Modified Carbon Nanofiber/UHMWPE Nanocomposite Films, *Macromolecules* 38 (2005) 3883.
- [2.23] CHOI S., CHUNG D., KWEN H., Fabrication of Biosensors Using Vinyl Polymer-grafted Carbon Nanotubes. *Intech Open Science*, 12 (2001) 245.
- [2.24] PING X., WANG M., GE X., Surface modification of poly(ethylene terephthalate) (PET) film by gamma-ray induced grafting of poly(acrylic acid) and its application in antibacterial hybrid film, *Radiat. Phys. Chem.* (2010) 1.
- [2.25] SAMMALKORPI M. et al, Irradiation-induced stiffening of carbon nanotube bundles, *Nucl. Instrum. Methods B* 228 (2005) 142.
- [2.26] TSOBOKAWA N. Functionalization of Carbon Material by Surface Grafting of Polymers, *Chem. Soc. Jpn.* 75 (2002) 2115.
- [2.27] EVORA M.C., KLOSTERMAN D., LAFDI K., LI.L., ABOT J.L., Functionalization of carbon nanofiber through electron beam radiation, *Carbon* 48 (2010) 2937.
- [2.28] JUNG C. et al., Surface functionalization of single-walled carbon nanotubes by a radiation grafting, *Appl. Chem.* 13 1 (2009), 25.
- [2.29] FILIK J., MAY P.W., PEARCE S.R.J., WILD R.K., HALLAM H.R, XPS and laser Raman analysis of hydrogenated amorphous carbon films, *Diamond and related materials* 12 (2003) 974.
- [2.30] ZHU Y., TANG J., ZHU W., ZHANG M., LIU G., LIU Y., ZHANG W., JIA M, Graphite oxide-supported CaO catalysts for transesterification of soybean oil with methanol *Bioresource Technology* 102 (2011) 8939.
- [2.31] HAN H. S., YOU J., JEONG H., JEON S., Synthesis of graphene oxide grafted poly(lactic acid) with palladium nanoparticles and its application to serotonin sensing, *Applied Surface Science* 284 1 (2013) 438.
- [2.32] TURGEON S., PAYNTER R.W., On the determination of carbon  $sp^2/sp^3$  ratios in polystyrene/polyethylene copolymers by photoelectron spectroscopy, *Thin Solid Films* 394, (2001) 44.
- [2.33] CHEN J., MAEKAW, Y., YOSHIDA M., TSOBOKAWA N., Radiation grafting of polyethylene onto conductive carbon black and application as a novel gas sensor, *Polym. J.* 34, n 1 (2002) 30.
- [2.34] FERRARI, A., Raman spectroscopy of graphene and graphite: Disorder, electron-phononcoupling, doping and nanodiabatic effect, *Solid State Commun.* 143 (2007) 47.